

## **An investigation of the influence of splitter plates on the vortical wake behind a circular cylinder in cross-flow**

B. G. Chierigatti<sup>1</sup>, B. S. Carmo<sup>1</sup>, E. V. Volpe<sup>1</sup>

<sup>1</sup> Department of Mechanical Engineering, Polytechnic School at the University of São Paulo

**Abstract.** *Widely recognized for its simplicity, the splitter plate is an effective device for drag reduction in bluff bodies. It consists of a flat plate, which is placed in the center line of the wake, in streamwise direction, and it works by changing the way the shear layers interact with one another. This paper analyzes the sensitivity the drag force exhibits with respect to the length and position of that simple device. The main purpose is to determine the plate dimensions that lead to a minimum of the time-averaged drag coefficient. The results agree with previously published data, to the effect that the extrema depend on the Reynolds number. Moreover, they show that minimum drag configurations may also be characterized by significant reductions in the amplitude of drag and lift oscillations.*

**Keywords:** *oil risers, splitter plate, drag reduction, optimization.*

## **1. INTRODUCTION**

Long flexible risers are essential components of drilling derricks in deep water oil extraction. Their usually bluff cross-sections lead to extensive regions of separated flow. As a result, they shed vortical wakes and are prone to vortex-induced vibrations, at all but the lowest Reynolds numbers. Add to it the fact that far-field flow conditions are ultimately determined by the swell and ocean tides, thereby remaining beyond any possibility of control.

Under such circumstances, a deep understanding of the physics of this class of flows is clearly of utmost importance to the oil industry. It has made it a most prolific research topic. Much attention has also been devoted to means of controlling bluff body flows. The possibilities range from active measures, such as forced oscillations [Meneghini and Bearman, 1995, Meneghini, 2002, Bearman and Currie, 1979, Feng, 1968], to passive devices such as trip-wires, vortex generators and splitter-plates.

Its easy assembly and operation gives the splitter plate an important advantage over many other flow control devices. In principle, it works by extending the length over which the shear layers on each side of a cylinder are separated. It delays the interaction between them, which has the effect of reducing the form drag significantly. In a seminal article on the problem, Igarashi [Igarashi, 1982] classifies the splitter plates according to the way they are assembled, relative to the cylinder. There are configurations in which the plate is attached to the cylinder, and others in which there is a gap between the two.

The contribution of the present work is an investigation of both cases, with and without gap, in a systematic attempt to find configurations that yield minimum form drag. The exploratory tests have been performed by means of numerical flow simulations, only. Incidentally, it may be useful to settle the definitions of the dimensionless parameters early on. The Reynolds ( $Re$ ) and Strouhal ( $St$ ) numbers, the pressure ( $C_p$ ), lift ( $C_l$ ) and drag ( $C_d$ ) coefficients are defined as, respectively,

$$\left\{ \begin{array}{l} Re = \frac{U_\infty L}{\nu} \\ St = \frac{fL}{U} \\ q_\infty = \frac{1}{2}\rho_\infty U_\infty^2 \end{array} \right. \quad \left\{ \begin{array}{l} C_p = \frac{p-p_\infty}{q_\infty} \\ C_l = \frac{\|l\|}{q_\infty L} \\ C_d = \frac{\|d\|}{q_\infty L} \end{array} \right. \quad (1)$$

For the sake of completeness:  $\nu$  is the fluid kinematic viscosity,  $\rho_\infty$  and  $U_\infty$  are free-stream density and velocity, respectively. The symbol  $f$  represents a frequency, which is taken here to be the vortex shedding frequency,  $U$  is another velocity scale, which is often taken to be  $U_\infty$ , itself, and  $L$  is a length scale that depends on the context.

## 2. LITERATURE SURVEY

For all their relevance in nature and engineering, separated flows are the object of extensive research and a prolific literature, in the realm of fluid mechanics. An inherent complexity has favored the experimental approach in the early years. More recently, though, the development of robust methods of numerical simulation has given rise to an ever-growing field in CFD that is entirely devoted to the topic. This survey attempts to follow the chronology.

In two of the earlier studies on the topic, Roshko has made a semi-empirical analysis of the flow around bluff bodies [Roshko, 1954a, Roshko, 1954b]. The reports did include cylinders with splitter plates, with and without gaps between them ( $Re = 1.45 \times 10^4$ ). Amongst their most relevant findings, the first one shows that the splitter plate changes the  $C_p$  distribution all over the cylinder surface, as opposed to affecting only the separated region. The second one shows that the dimensionless frequency of vortex shedding ( $St$ ) decreases as the gap grows, up until a critical value is reached. After this value, the  $St$  jumps back up to a value that is close to that of the isolated cylinder. The cylinder base pressure ( $C_{pb}$ ) exhibits a similar behavior, with the only difference that it grows slightly just before the gap reaches the critical value, only to decrease afterwards. The critical size of the gap is identified as the point where the vortex formation region moves from the trailing edge of the plate to the gap itself.

In an experimental study on bodies with splitter plates, [Bearman, 1965] presents results for  $C_{pb}$ ,  $St$  and velocity fluctuations in the wake, for  $Re$  in the range:  $1.4 \times 10^5 \leq Re \leq 2.56 \times 10^5$ . Among many important results, he has found that the value of  $-C_{pb}$  is inversely proportional to the so-called *vortex formation length* ( $l_f$ )— which was then defined as the  $x$  coordinate of the point on the wake axis, where the  $rms$ <sup>1</sup> of velocity fluctuations peaks.

---

<sup>1</sup>acronym for root mean square

A paper by Gerrard [Gerrard, 1966] investigated the physics of the vortex formation region behind bluff bodies. He suggested the key mechanism in vortex formation is the mutual-interaction between the two shear layers, which arise from boundary layer separation on each side of the cylinder. Furthermore, he proposed that vortex shedding takes place because of fluid entrainment from one layer into the other, in a scheme that is best depicted by his classic sketch—which we took the liberty of reproducing below (fig. 1–left), for clarity.

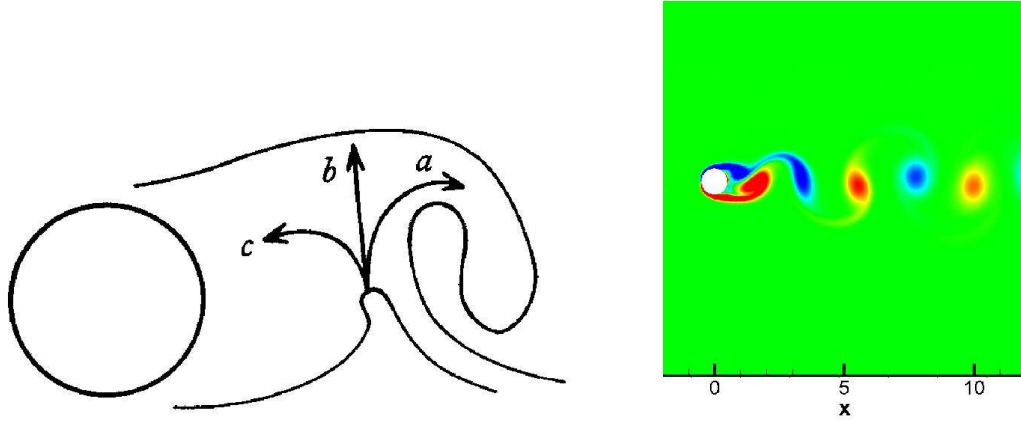


Figure 1. Left, the mechanism of vortex formation behind a circular cylinder, in an excerpt from Gerrard [Gerrard, 1966]. Rolling-up of the shear layers is indicated by filament lines, and the arrows show the fluid path afterwards. Right, a numerical simulation of the same problem, which effectively shows the vortex wake behind the cylinder ( $Re = 100$ ).

It is well-known that the fluid on each shear layer bears vorticity of opposite sign. Under this condition, the filament lines show the shear layers rolling up and the arrows indicate the fluid path afterwards. Part of it is entrained by the growing vortex (*a*). Another part (*b*) is entrained by the upper shear layer and, on bearing opposite vorticity, it helps to cut the forming vortex off. A third part (*c*) flows toward the formation region, where it feeds into the lower vortex formation. The formation length  $l_f$  is defined here as the point at which the fluid from outside the wake first crosses its axis.

In [Gerrard, 1966], the author performed experiments on cylinders with splitter plates, with and without gaps, and has also reproduced some of Roshko experiments ( $Re = 2 \times 10^4$ ). On doing so, he was able to verify and explain some of Roshko's claims, such as the discontinuity in  $St$  that happens as  $l_f$  moves from the plate trailing edge to within the gap.

In [Apelt et al., 1973], the authors run a set of experiments involving splitter plates fixed to the basis of the cylinder, for  $Re$  in the range:  $10^4 \leq Re \leq 5 \times 10^4$ . The length  $l/d = 1$  was set as a limit to differentiate between long and short splitter plates. They found that short plates diminish the width of the wake and stabilize the boundary layer separation points on the cylinder, thus causing the vortices to form closer to the plate trailing edge. On the other hand, long plates inhibit the interaction between shear layers, thus causing vortices to form farther away from the plate. A sequence to their research was published in [Apelt et al., 1975].

A paper by Igarashi, from 1982 [Igarashi, 1982], reports on extensive experimental research into cylinders with splitter plates. The sizes of the plates and gaps varied within the ranges  $0.29 \leq l/d \leq 1.76$  and  $0 \leq g/d \leq 4$ , respectively, while the Reynolds number was

kept:  $1.3 \times 10^4 \leq Re \leq 5.8 \times 10^4$ . The results show the variations of shedding frequency ( $St$ ), base pressure ( $C_{pb}$ ) and drag ( $C_d$ ) with respect to gap and plate sizes. Special emphasis is placed upon the discontinuity that appears as the vortex formation moves from the plate trailing edge to within the gap. He also classified previous works on the topic into three groups, according to their motivations. A first group is primarily concerned with the universal dimensionless frequencies ( $St$ ) of vortex shedding [Roshko, 1954a, Roshko, 1954b, Gerrard, 1966]. A second group is concerned with the way the plate affects the flow field and, hence, with its effects on lift and drag [Bearman, 1965, Apelt et al., 1973, Apelt et al., 1975]. Finally, a third group focuses on the heat transfer characteristics of the turbulent separated flow region behind the cylinder, as is the case of a later work of his [Igarashi, 1984].

Two articles by Unal and Rockwell on the topic were published six years after Igarashi [Unal and Rockwell, 1988a, Unal and Rockwell, 1988b]. The first one explores the hydrodynamic instabilities that appear in the flow around a cylinder at lower Reynolds ( $440 \leq Re \leq 5040$ ). The second one analyzes the case of a very long splitter plate,  $l/d = 24$ , at various gaps,  $0 \leq g/d \leq 15$ . With regard to the frequencies of velocity fluctuations in the wake, their results have been interpreted as indicative of the thesis that the splitter plate inhibits the vortex shedding, but it does not inhibit the shear layers instability.

In [Kawai, 1990], the author performed numerical simulations of flow around cylinders with splitter plates of various lengths and gaps. He made use of the discrete vortex method, and his results exhibit the same characteristics as those from Roshko and Apelt. However, his numerical values were different—in particular, the critical gap was about half of the corresponding experimental value. However, the differences have been attributed to differences in the Reynolds number that had been prescribed for the simulations.

A more recent paper by Kwon and Choi [Kwon and Choi, 1996], presents numerical simulations at lower Reynolds numbers ( $80 \leq Re \leq 160$ ). They only considered cases where the splitter plate is fastened to the cylinder. The paper analyzes the behavior of the Strouhal number ( $St$ ) with changing  $Re$  and different plate lengths. Their results are similar to those obtained by Gerrard and Apelt, despite the fact that their simulations have been run at much lower Reynolds numbers.

From the same year, a paper by Nakamura [Nakamura, 1996] analyzes the vortex shedding mechanism for various kinds of bluff bodies, all with splitter plates fastened to their bases. The author has run experiments for  $Re$  between 300 and 500, and has made use of long plates. The paper reports on a gradual transition between two distinct modes of vortex shedding, as the plate length grows. The transition is from the usual mode, which involves mutual interaction between the shear layers, and a mode that is governed by the so-called impinging–shear-layer instability.

### 3. RESULTS

The idea that the drag decreases for certain arrangements of the splitter plate is fully consistent with most of the above references. As has been verified by experiment, it happens because the plate can extend the formation length of the wake, depending on its size and position relative to the cylinder. In principle, if there is no gap between cylinder and plate, one could attempt to enhance the effect by increasing the length of the latter. It is clear,

though, that the penalty of a growing viscous drag on the plate would eventually offset the benefit. In essence, then, the gap is an attempt at heaping up the benefits of an increased formation length, without incurring the penalty of higher friction drag on the plate.

On the other hand, most references point out that, as the gap exceeds a critical value, which corresponds to minimum drag, the vortex formation region moves within it— it gets enclosed between cylinder and plate. That, in turn, causes the drag to increase abruptly, which thus limits the benefits of this particular device.

One of the references that is directly related to our objectives, [Igarashi, 1982] presents a large collection of experimental results for the flow around cylinders with splitter plates. On following in that author's footsteps, a series of numerical experiments have been performed. The idea was to reproduce his experiments to some extent, if not completely, and to ascertain how much of the flow physics could be captured by the simulations.

Owing to limitations of the numerical method, the values of  $Re$  were set in a range lower than his:  $80 \leq Re \leq 140$ . Two lengths of splitter plate ( $l$ ) relative to the cylinder diameter ( $d$ ) were set in the range:  $0.5 \leq (l/d) \leq 1.0$ . Whereas the relative size of the gap ( $g/d$ ), ranged from 0.0 to 4.0, where  $g$  measures the distance from the base of the cylinder to the leading edge of the splitter plate.

All simulations have been performed with the software NEKTAR, which is based on the spectral element method, with Galerkin weighed residuals. The tests have made use of polynomials of 7th order for base functions, and a 2nd order scheme for time stepping. The mesh had 516 elements, with origin at the center of the cylinder. It extended from  $-60 \times d$  to  $60 \times d$  in the streamwise direction ( $x$  coordinate), and from  $-50 \times d$  to  $50 \times d$  in the normal direction ( $y$  coordinate). These arrangements were defined on the basis of a recent report [Serson and Meneghini, 2010], in which the authors had run a thorough investigation on grid-independence and simulation accuracy, with the same code and for the same class of flows.

No-slip boundary conditions have been imposed on the cylinder wall, while the splitter plate was only imposed the condition  $\mathbf{u} \cdot \mathbf{n} = 0$ . Hence, the tests do not account for viscous stresses on the plate, nor do they consider the viscous drag thereof, Although the forces on the cylinder are fully accounted for. This setup is fairly general practice in the CFD community, regarding this class of flows, because it allows a very significant reduction in computational costs. However, it does make for an important difference between numerical and experimental results.

For the purpose of comparison, for each case with a splitter plate, a corresponding test was run without it, under the same flow conditions. As an example, figure 1–right, shows contours of vorticity of the flow around a cylinder without splitter plate, at  $Re = 100$ . As an illustration of the effects the splitter plate has on the flow, fig. 2 presents vorticity contours for different lengths of splitter plates, all with zero gap ( $g/d = 0$ ). It shows that the wake formation length ( $l_f$ ) grows with the plate length.

The effects of the gap are depicted in fig. 3. It presents a sequence of tests where the plate length has been kept constant at  $l/d = 1.0$ , while the gap was increased from 1.2 to 2.8. The first and second pictures, from left to right, show similar behavior to the zero gap case, in that  $l_f$  grows with the spacing between the basis of the cylinder and the plate trailing edge,

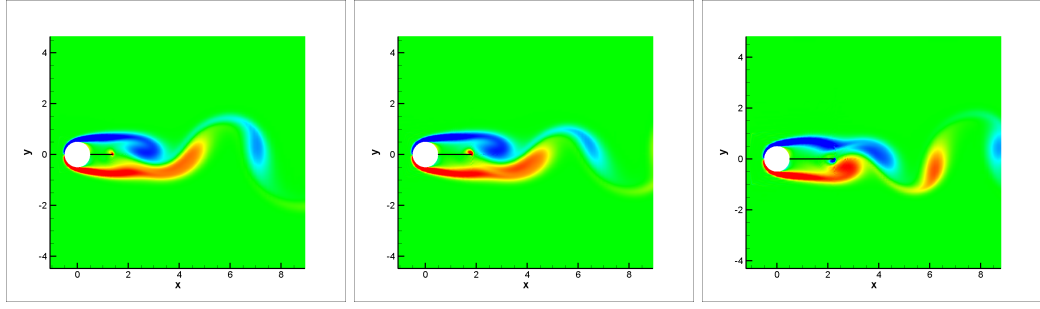


Figure 2. Contours of vorticity of the flow around a cylinder with splitter plate. 2-D flow solutions for different lengths  $a/d$ , all of them with no gap between plate and cylinder, at  $Re = 100$ . From left to right: 1st,  $l/d = 0.8$ ; 2nd,  $l/d = 1.4$ ; 3rd,  $l/d = 1.8$ .

$(g + l)/d$ . Quite a different result is seen in third picture, though. There the gap has grown larger than the formation region, which now lies within it.

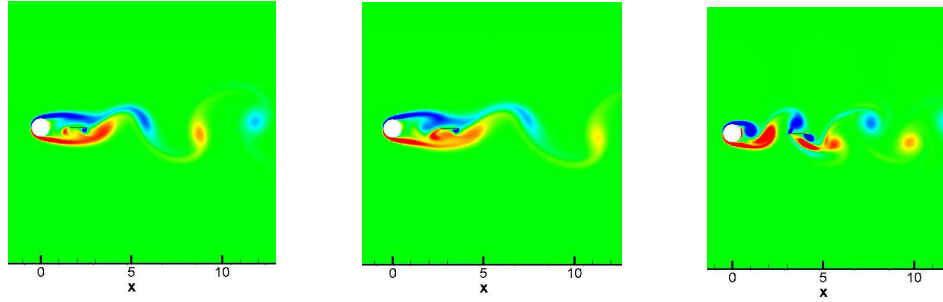


Figure 3. Contours of vorticity of the flow around a cylinder with splitter plate. 2-D flow solutions for different gaps  $g/d$ , all of them with the same length  $l/d = 1.0$ , at  $Re = 100$ . From top to bottom, left to right: 1st,  $g/d = 1.2$ ; 2nd,  $g/d = 2.6$ ; 3rd,  $g/d = 2.8$ .

The above changes in the wake structure clearly affect drag and lift forces alike. The unsteady nature of the flow imparts oscillations to the forces— where the latter must have zero mean, owing to flow symmetry. Figure 4 illustrates these effects in time domain, for the case where  $l/d = 1$ , while  $g/d$  is increased from 0.2 to 4.0, all at  $Re = 100$ .

In fig. 4-left, it is clear that  $C_l$  oscillates with zero mean, as was expected. Furthermore, one sees that not only does the amplitude decrease as the gap grows, but so does the frequency. The trends persist up to a critical point, which represents a minimum for both amplitude and frequency. If the gap grows beyond that point, then both parameters jump back to the same orders of magnitude they exhibit for an isolated cylinder. The same trends can be noticed in fig. 4-right, which shows the  $C_d$  evolution. Only, in this case, time averages are clearly nonzero, and it can be seen that the mean  $C_d$  also reaches a minimum at the same critical value of  $g/d$ , beyond which it experiences large growth.

In an attempt to give a more systematic view of the results, for different values of  $Re$ ,  $l/d$  and  $g/d$ , we picked parameters that should be representative of the periodic flow. To that end, the drag coefficient has been time-averaged over 10 periods of regular oscillations ( $\overline{C_d}$ ), while the lift coefficient evolution is represented by the maximum amplitude of its oscillations

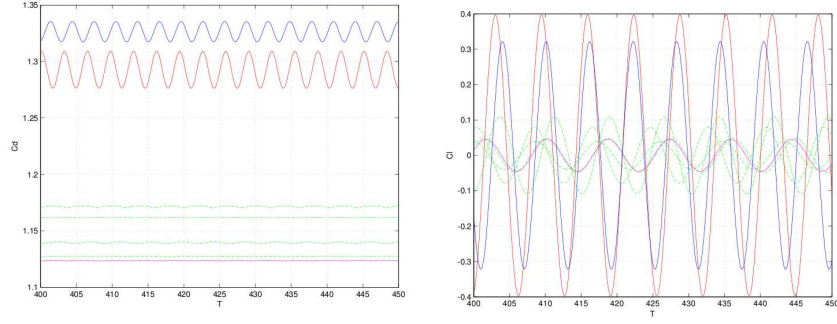


Figure 4. Time dependence of  $c_d$  (left) and  $c_l$  (right) for different  $g/d$ , at  $Re = 100$ ,  $l/d = 1.0$ . Blue solid line, no splitter plate. Magenta solid line,  $g/d = 2.6$ , which minimizes the time averaged  $C_d$ . Green dash-dot lines, intermediary values of  $g/d$ . Red solid line, value of  $g/d$  that exceeds formation length, thus allowing shear layers to interact within the gap.

over the same time-span. In addition to that, the Strouhall number ( $St$ ) and formation length ( $l_f$ ) are plotted against gap ( $g/d$ ), as part of the analysis.

Figure 5 compares an isolated cylinder to cylinders with splitter plates, but no gap, with respect to values of  $\overline{C_d}$  and  $C_l$  maximum amplitude. Various plate lengths are considered. It can be seen, the plate can reduce the time-averaged drag up to 20.5%, and diminishes the  $C_l$  amplitude by up to 42.8%.

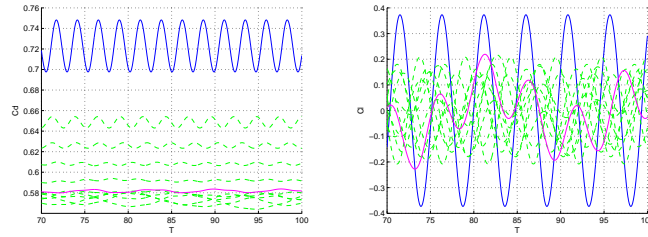


Figure 5. Time-averaged  $\overline{C_d}$  and  $C_l$  amplitude for the zero gap configuration as functions  $l/d$ , at  $Re = 100$ . Red dash-dot lines, no splitter plate. Blue dash-dot lines, with splitter plate. Left,  $\overline{C_d} \times l/d$ ; right,  $C_l$  amplitude  $\times l/d$ .

As it is pointed out by [Igarashi, 1982], experimental results show the mean drag reaches a minimum at a certain plate length. Beyond that, the value of  $\overline{C_d}$  grows back, as a result of an increasing viscous drag on the plate itself, thus offsetting its original benefit. In the above results,  $\overline{C_d}$  is shown to level off, instead. As we mentioned above, the behavior is owed to the fact that the viscous drag on the plate has been neglected.

Figures 6–7 bring results for  $\overline{C_d}$  and maximum  $C_l$  amplitude in a set of tests, for two distinct plate lengths:  $l/d = 0.5$  and  $l/d = 1.0$ , respectively; all at  $Re = 100$ . These tests have focused on the dependence of  $\overline{C_d}$  and  $C_l$  amplitude on the gap size  $g/d$ , for a fixed  $Re$ .

The results show the mean drag can be reduced by up to 11.2% for  $l/d = 0.5$  and by 15.7% for  $l/d = 1.0$ . It is also clear that, in all cases, on increasing the gap just beyond the

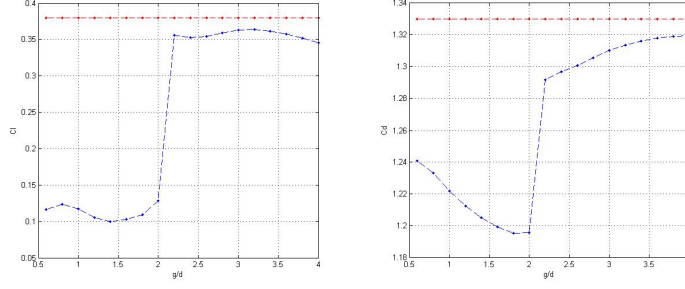


Figure 6. Maximum amplitude of  $C_l$  and  $\overline{C_d}$  versus  $g/d$ , at  $Re = 100$  and  $l/d = 0.5$ . Red dash-dot lines, no splitter plate. Blue dash-dot lines, with splitter plate. Left,  $\overline{C_d}$ ; right,  $C_l$  maximum amplitude.

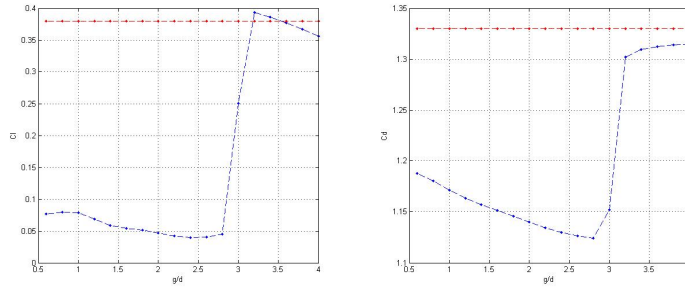


Figure 7. Maximum amplitude of  $C_l$  and  $\overline{C_d}$  versus  $g/d$ , at  $Re = 100$  and  $l/d = 1.0$ . Red dash-dot lines, no splitter plate. Blue dash-dot lines, with splitter plate. Left,  $\overline{C_d}$ ; right,  $C_l$  maximum amplitude.

point of minimum  $\overline{C_d}$ , that coefficient undergoes a sharp jump discontinuity, thus reaching values that are close to that of the isolated cylinder. The jump is an immediate result of the fact the vortex formation region has moved into the gap. As for the maximum amplitude of  $C_l$  oscillations, the device reduces it by up to 73.0% in the first case and 89.1% in the second.

It must also be noted that the values of  $g/d$  that lead to minimum  $\overline{C_d}$  and minimum  $C_l$  amplitude for each case are either coincident or very close to it. Moreover, the behavior of the  $C_l$  amplitude strongly resembles that of  $\overline{C_d}$ , in that both grow rapidly beyond their minimum. These features are further evidence that the vortex formation length virtually controls the physics of this class of flows. In that sense, it is noteworthy that the numerical simulations could capture such substantial part of the physics, despite the neglect of viscous stresses on the plate.

The exact same trends are verified for other values of the Reynolds number, such as  $Re = 80$ , and  $Re = 140$ . The results are shown in the sets of figures. 8–9 and 10–11, respectively.

Test results for  $Re = 80$  show the  $\overline{C_d}$  can be reduced by up to 6.3% for  $l/d = 0.5$  and by 12.0% for  $l/d = 1.0$ , the maximum amplitude of  $C_l$  oscillations decreases by 80.0% and 94.0% respectively.



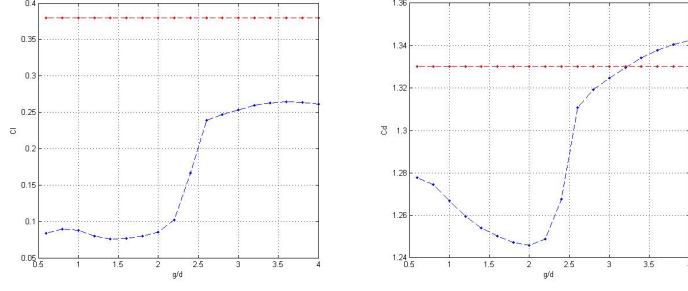


Figure 8. Maximum amplitude of  $C_l$  and  $\overline{C_d}$  versus  $g/d$ , at  $Re = 80$  and  $l/d = 0.5$ . Red dash-dot lines, no splitter plate. Blue dash-dot lines, with splitter plate. Left,  $\overline{C_d}$ ; right,  $C_l$  maximum amplitude.

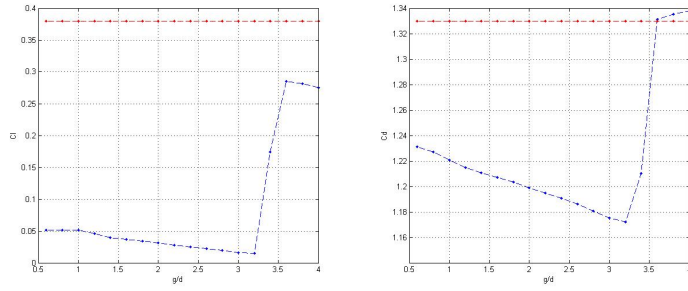


Figure 9. Maximum amplitude of  $C_l$  and  $\overline{C_d}$  versus  $g/d$ , at  $Re = 80$  and  $l/d = 1.0$ . Red dash-dot lines, no splitter plate. Blue dash-dot lines, with splitter plate. Left,  $\overline{C_d}$ ; right,  $C_l$  maximum amplitude.

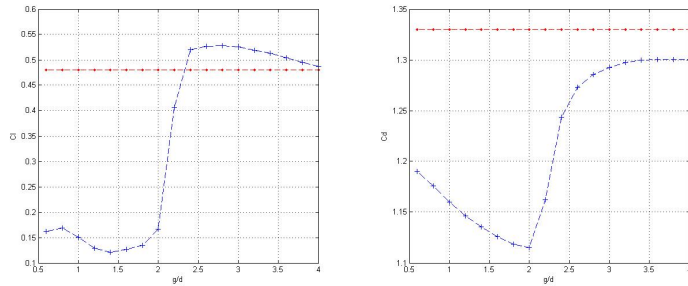


Figure 10. Maximum amplitude of  $C_l$  and  $\overline{C_d}$  versus  $g/d$ , at  $Re = 140$  and  $l/d = 0.5$ . Red dash-dot lines, no splitter plate. Blue dash-dot lines, with splitter plate. Left,  $\overline{C_d}$ ; right,  $C_l$  maximum amplitude.

For the case with  $Re = 140$ , the reduction in  $\overline{C_d}$  is of about 13.5% for  $l/d = 0.5$  and of 23.3% for  $l/d = 1.0$ . While the maximum amplitude of  $C_l$  oscillations is diminished by about 74.7% and 92.1%, respectively. Here again, the results are of the same order of magnitude as the previous cases.

On comparing results for the same plate length, at different Reynolds numbers, one

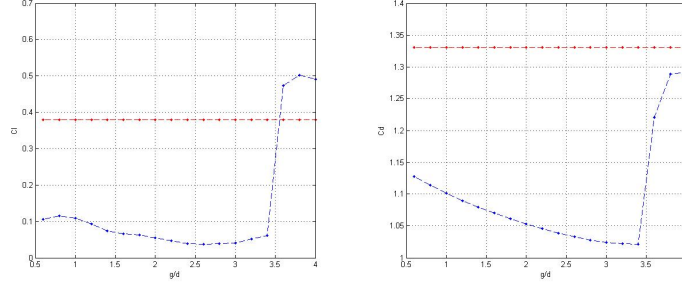


Figure 11. Maximum amplitude of  $C_l$  and  $\overline{C_d}$  versus  $g/d$ , at  $Re = 140$  and  $l/d = 1.0$ . Red dash-dot lines, no splitter plate. Blue dash-dot lines, with splitter plate. Left,  $\overline{C_d}$ ; right,  $C_l$  maximum amplitude.

notices that the value of  $g/d$  for minimum  $\overline{C_d}$  diminishes with growing  $Re$ . In a sense, the trend is consistent with the case of an isolated cylinder, for which higher values of  $Re$  are known to lead to smaller formation lengths [Serson and Meneghini, 2010]. A different picture emerges when comparing gap sizes for different  $l/d$  at the same  $Re$ . That comparison shows the value of  $g/d$  that yields minimum  $\overline{C_d}$  grows with the relative length.

The effects of the gap size on the Strouhal number ( $St$ ), for different  $Re$ , at a fixed plate length,  $l/d = 0.5$ , are depicted in fig. 12. It must be noted that  $St$  has been defined here on the basis of the vortex shedding frequency, free-stream velocity and cylinder diameter. A similar analysis is presented in fig. 13 for the case where  $l/d = 1.0$ . The same trends are seen in all cases, in that there is a pronounced decrease in  $St$  with growing  $g/d$ . As the gap is increased beyond the point of minimum, the Strouhal number grows steeply, only to reach values that are closer to that of the isolated cylinder. However, the most remarkable feature of these results lies in the fact that the point of minimum vortex shedding frequency coincides with the point of minimum mean drag  $\overline{C_d}$  and minimum amplitude of  $C_l$  oscillations.

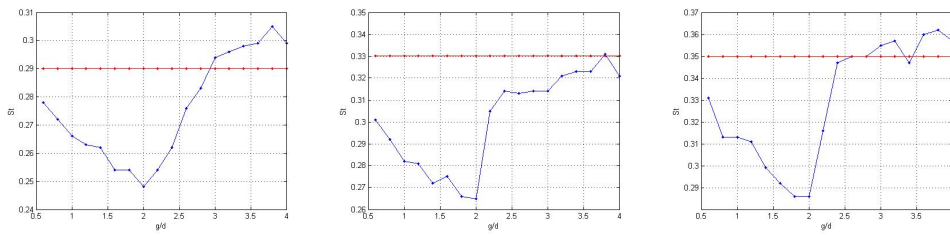


Figure 12. Strouhal number  $St$  versus gap size  $g/d$ , for  $l/d = 0.5$ . Left,  $Re = 80$ ; center,  $Re = 100$ ; right,  $Re = 140$ . Red dash-dot lines, no splitter plate; blue dash-dot lines, with splitter plate.

Figures 14 and 15 show the effects of the gap size on the vortex formation length ( $l_f$ ), for two sizes of splitter plate:  $l/d = 0.5$  and  $l/d = 1.0$ , respectively. The parameter  $l_f$  has been defined here as the  $x$  coordinate of the first point on wake axis ( $y = 0$ ) where the time-averaged  $x$  component of the flow velocity goes through zero. The figures bring the parameter in dimensionless form, that is:  $l_f/d \propto g/d$ .

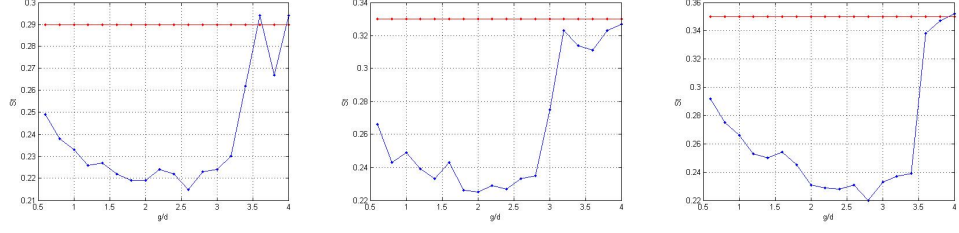


Figure 13. Strouhal number  $St$  versus gap size  $g/d$ , for  $l/d = 1.0$ . Left,  $Re = 80$ ; center,  $Re = 100$ ; right,  $Re = 140$ . Red dash-dot lines, no splitter plate; blue dash-dot lines, with splitter plate.

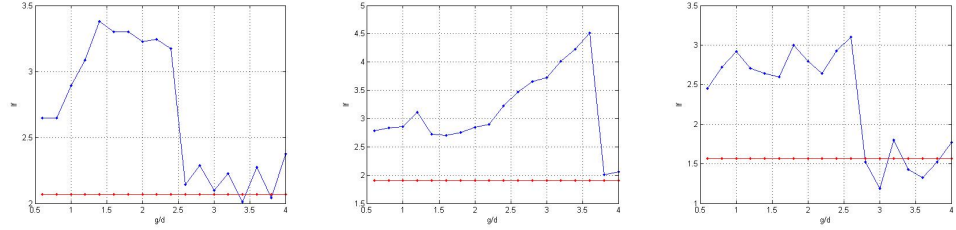


Figure 14. Dimensionless formation length  $l_f/d$  versus gap size  $g/d$ , for  $l/d = 0.5$ . Left,  $Re = 80$ ; center,  $Re = 100$ ; right,  $Re = 140$ . Red dash-dot lines, no splitter plate; blue dash-dot lines, with splitter plate.

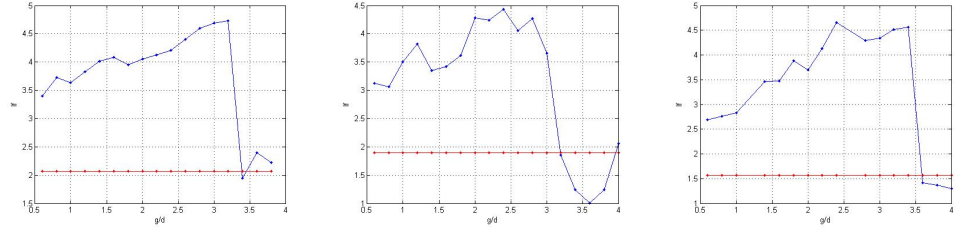


Figure 15. Dimensionless formation length  $l_f/d$  versus gap size  $g/d$ , for  $l/d = 1.0$ . Left,  $Re = 80$ ; center,  $Re = 100$ ; right,  $Re = 140$ . Red dash-dot lines, no splitter plate; blue dash-dot lines, with splitter plate.

The above results corroborate the hypothesis that the formation length controls this class of flows. For they show  $l_f/d$  grows with  $g/d$  up to a maximum, which corresponds to the minimum values of  $\overline{C_d}$ ,  $C_l$  amplitude and  $St$ . In the ascent, the flow physics is such that  $l_f/d \geq (g + l)/d$ . When the gap is increased beyond the point of maximum  $l_f$ , it falls to levels that are comparable to that of the isolated cylinder. In essence, that implies the vortex formation region gets contained within the gap,  $l_f/d \leq g/d$ .

For completeness figs. 16 and 17 present the pressure coefficient at the base of the cylinder versus gap size ( $-C_{pb} \times g/d$ ) for  $l/d = 0.5$  and  $l/d = 1.0$ , respectively. Here, it is understood that  $C_{pb}$  is based on a time-average of pressure over a time-span of 10 regular periods, and the base corresponds to the point  $(x, y) = (d/2, 0)$ , where the origin is at the

center of the cylinder and the  $x$  axis is oriented downstream.

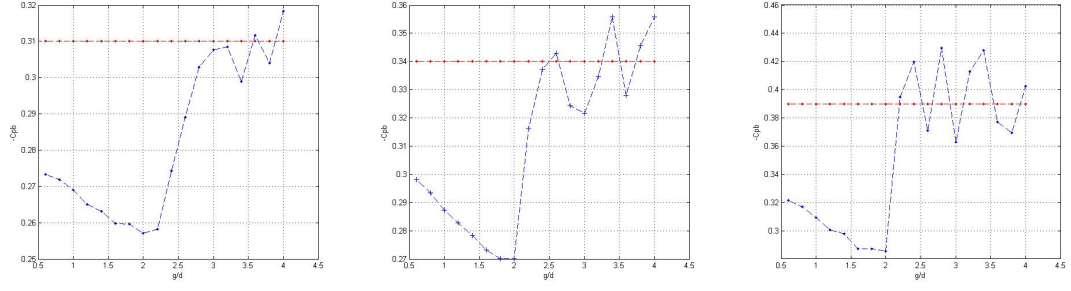


Figure 16. Base Pressure Coefficient  $-C_{pb}$  versus gap size  $g/d$ , for  $l/d = 0.5$ . Left,  $Re = 80$ ; center,  $Re = 100$ ; right,  $Re = 140$ . Red dash-dot lines, no splitter plate; blue dash-dot lines, with splitter plate.

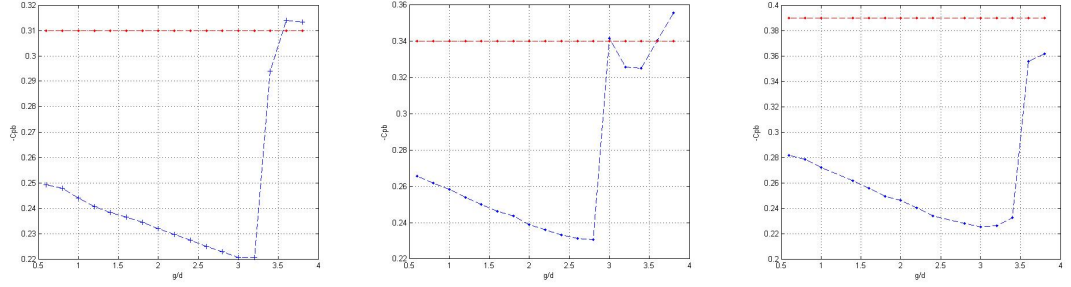


Figure 17. Base Pressure Coefficient  $-C_{pb}$  versus gap size  $g/d$ , for  $l/d = 1.0$ . Left,  $Re = 80$ ; center,  $Re = 100$ ; right,  $Re = 140$ . Red dash-dot lines, no splitter plate; blue dash-dot lines, with splitter plate.

As is widely reported in the literature,  $-C_{pb}$  shows strong correlation with the corresponding form drag,  $\overline{C_d}$ . The results give further evidence of the accuracy of the numerical simulations, which have been performed here.

#### 4. CONCLUDING REMARKS

A systematic investigation has been performed into the flow around a circular cylinder with a wake splitter plate. A number of numerical have been carried out, considering various plate lengths and gap sizes. The Reynolds number has been set at values within the range  $80 \leq Re \leq 140$ , and the flow model was substantially simplified, in that viscous stresses on the splitter plate have been neglected.

In spite of the simplification, the results have shown to capture such relevant aspects of the flow physics, like discontinuity the vortex formation length experiences, as a function of the gap size. That discontinuity is characterized by a finite jump, which is owed to the transition of the vortex formation region from downstream of the plate to within the gap. The jump is preceded by the maximum formation length, and that same extremum is also associated

with minimum values for the time-averaged form-drag, amplitude of lift oscillations, and vortex shedding frequency. Yet, our results suggest its dependence on the Reynolds number may be stronger in this range, than it had been anticipated in previous works.

With regard to potential applications the device has in the oil industry, that extremum truly represents the optimum configuration. However, its dependence on the Reynolds number prompts the need for further analysis, and may entail compromise solutions. After all, that parameter is naturally beyond control in oceanic systems.

## 5. REFERENCES

### References

- [Apelt et al., 1973] Apelt, C. J., West, G. S., and Szewczyk, A. A., 1973, The effects of wake splitter plates on bluff-body flow in the range  $10^4 < R < 5 \times 10^4$ ., “Journal of Fluid Mechanics”, Vol. 61, No. 1, pp. 187–198.
- [Apelt et al., 1975] Apelt, C. J., West, G. S., and Szewczyk, A. A., 1975, The effects of wake splitter plates on bluff-body flow in the range  $10^4 < R < 5 \times 10^4$ . Part 2., “Journal of Fluid Mechanics”, Vol. 71, No. 1, pp. 145–160.
- [Assi et al., 2009] Assi, G. R., Bearman, P. W., and Kitney, N., 2009, Low drag solutions for suppressing vortex-induced vibration of circular cylinders, “Journal of Fluids and Structures”, Vol. 25, No. 4, pp. 666–675.
- [Bearman, 1965] Bearman, P. W., 1965, Investigation of the flow behind a two-dimensional model with a blunt trailing edge and fitted with splitter plates, “Journal of Fluid Mechanics”, Vol. 21, No. 2, pp. 241–255.
- [Bearman and Currie, 1979] Bearman, P. W. and Currie, I. G., 1979, Pressure fluctuation measurements on an oscillating circular cylinder, “Journal of Fluid Mechanics”, Vol. 91, No. 4, pp. 661–667.
- [Feng, 1968] Feng, C. C., 1968, The measurement of vortex-induced effects in a flow past stationary and oscillating circular and D-section cylinders, M.sc. thesis, University of British Columbia, Canada.
- [Gerrard, 1966] Gerrard, J., 1966, The mechanics of the formation region of vortices behind bluff bodies, “Journal of Fluid Mechanics”, Vol. 25, No. 2, pp. 401–413.
- [Igarashi, 1982] Igarashi, T., 1982, Investigation on the Flow behind a Circular Cylinder with a Wake Splitter Plate, “Bulletin of the JSME”, Vol. 25, No. 202, pp. 528–535.
- [Igarashi, 1984] Igarashi, T., 1984, Correlation between heat transfer and fluctuating pressure in separated region of a circular cylinder, “International Journal of Heat and Mass Transfer”, Vol. 27, No. 6, pp. 927–937.
- [Kawai, 1990] Kawai, H., 1990, Discrete vortex simulation for flow around a circular cylinder with a splitter plate, “Journal of Wind Engineering and Industrial Aerodynamics”, Vol. 33, No. 1.
- [Kwon and Choi, 1996] Kwon, K. and Choi, H., 1996, Control of laminar vortex shedding behind a circular cylinder using splitter plates, “Physics of Fluids”, Vol. 8, No. 2, pp. 479–486.

- [Meneghini, 1993] Meneghini, J. R., 1993, “Numerical Simulation of Bluff Body Flow Control Using a Discrete Vortex Method”, PhD thesis, Imperial College of Science, Technology and Medicine, University of London, London, UK.
- [Meneghini, 2002] Meneghini, J. R., 2002, Geração e Desprendimento de Vórtices no Escoamento ao Redor de Cilindros, Tese de livre docência, Escola Politécnica da Universidade de São Paulo, São Paulo.
- [Meneghini and Bearman, 1995] Meneghini, J. R. and Bearman, P. W., 1995, Numerical simulation of high amplitude oscillatory flow about a circular cylinder, “Journal of Fluids and Structures”, Vol. 9, pp. 435–455.
- [Nakamura, 1996] Nakamura, Y., 1996, Vortex shedding from bluff bodies with splitter plates, “Journal of Fluid and Structures”, Vol. 10, No. 2, pp. 147–158.
- [Roshko, 1954a] Roshko, A., 1954a, On the development of turbulent wakes from vortex streets, Report 1191, NACA.
- [Roshko, 1954b] Roshko, A., 1954b, On the drag and shedding frequency of two-dimensional bluff bodies, Technical Note 3169, NACA.
- [Serson and Meneghini, 2010] Serson, D. and Meneghini, J. R., 2010, Simulações Numéricas do Escoamento ao redor de um Cilindro com Splitter Plate, Research Report 1, Escola Politécnica da Universidade de São Paulo, Brazil, Projeto FAPESP 2009/14233–1.
- [Shukla et al., 2009] Shukla, S., Govardhan, R. N., and Arakeri, J. H., 2009, Flow over a cylinder with a hinged-splitter plate, “Journal of Fluids and Structures”, Vol. 25, No. 4, pp. 713–720.
- [Unal and Rockwell, 1988a] Unal, F. M. and Rockwell, D., 1988a, On vortex formation from a cylinder. Part 1. The initial instability., “Journal of Fluid Mechanics”, Vol. 190, pp. 491–512.
- [Unal and Rockwell, 1988b] Unal, F. M. and Rockwell, D., 1988b, On vortex formation from a cylinder. Part 2. Control by splitter-plate interference., “Journal of Fluid Mechanics”, Vol. 190, pp. 513–529.